of 0.04 for p in the $\sigma(I)$ equation.[17] The final difference Fourier map did not reveal any chemically significant features. The CF_3 groups show some signs of minor disorder, but simple disorder models did not improve the structure. In light of the goals of the structure determination, this point was not further pursued.

The final atomic coordinates with their estimated standard deviations and the final thermal parameters are given in Table I. Note that the chemically equivalent atoms of the two independent $Pd(F_6acac)_2(PPh_3)$ molecules are labeled with unprimed and primed names. Tables of observed and calculated structure factor amplitudes are available as supplementary material. Figure 1 presents an ORTEP perspective of the molecular structure of the unprimed $Pd(F_6acac)_2(PPh_3)$ molecule and shows the labeling scheme. The labeling scheme for the primed molecule is identical.

Registry No. 1, 83220-99-9; **2**, 75810-99-0; **3**, 83221-01-6; **4**, 83221-02-7; **5**, 83221-03-8; **6**, 83221-04-9; **7**, 83221-06-1; **8**, 83221-07-2.

Supplementary Material Available: Listings of observed and calculated structure factor amplitudes (Table S1), anisotropic thermal parameters (Table S2), and least-squares planes (Table S3) and an appendix containing a theoretical analysis of the DNMR spectra (34 pages). Ordering information is given on any current masthead page.

Surface-Modified Photochemistry. Preparation of Silica-Supported $Fe_3(CO)_{12}$ via Irradiation of Adsorbed $Fe(CO)_5$

Robert L. Jackson* and Mark R. Trusheim

Contribution from the Corporate Research Center, Allied Corporation, Morristown, New Jersey 07960. *Received December 18, 1981*

Abstract: The photochemistry of silica-adsorbed $Fe(CO)_5$ has been studied. IR and UV-visible spectra show that the only significant product is $Fe_3(CO)_{12}$ rather than $Fe_2(CO)_9$, which is the product observed following irradiation of $Fe(CO)_5$ in the gas or liquid phase or in solution. Formation of $Fe_3(CO)_{12}$ is discussed in terms of a mechanism involving rapid secondary thermal reactions of a surface-complexed form of $Fe(CO)_4$.

Introduction

Research in transition-metal catalysis has increasingly turned toward catalyst systems based on metal carbonyl complexes and their derivatives. These systems have led to significant technological advances, as metal carbonyls have directly or indirectly provided active catalysts for a number of important processes.[1] While most of these processes are catalyzed homogeneously, metal carbonyl complexes have recently been used as precursors in the synthesis of supported heterogeneous catalysts.[2-7] This technique has a number of advantages over more conventional methods proceeding via the reduction of supported metal salts. Catalyst preparation can be simplified, since metal carbonyls are often sufficiently volatile to allow their deposition directly onto the support from the gas phase. Supported metal carbonyls can also be prepared from complexes of lower volatility by solution impregnation employing a low-boiling organic solvent. In addition, metal carbonyls are easily decomposed directly to the metal under rather mild conditions. High temperatures, as required in preparing supported transition-metal catalysts from metal nitrate or chloride salts, are thus unnecessary. This improves the chances of achieving high metal dispersions even at relatively high metal concentrations.

We have recently begun to explore the possibility of preparing supported transition-metal catalysts from metal carbonyl complexes using photochemical methods. There are a number of potential advantages in using light-initiated processes here, since metal carbonyl complexes possess a very rich photochemistry. For example, mononuclear carbonyl complexes can oligomerize upon irradiation.[8] It may be possible then to prepare supported polynuclear complexes in a single step by irradiating the mononuclear complex in the presence of the support material. Multiple deligandations of metal carbonyls to highly unsaturated complexes[9,10] or even metal atoms[11,12] can also be photochemically induced. This may allow direct preparation of very small supported metal clusters via photodeligandation of metal cluster complexes, thereby avoiding a thermal decomposition step which could induce sintering. There are obstacles, however, that have thus far limited application of photochemical methods to the preparation of supported transition-metal catalysts.[13] The most obvious is the opacity of many traditional oxide support materials. At best, this drastically reduces the efficiency of any photochemical process due to a nearly complete loss of useful light to scattering and reflection or to absorption by the support. We have avoided this problem by employing a rather transparent silica as our support. By irradiating $Fe(CO)_5$ adsorbed on this material, we have successfully prepared supported $Fe_3(CO)_{12}$ in a single-step process. We describe our results in the following sections and propose a mechanism whereby $Fe_3(CO)_{12}$ is produced from sec-

(1) Pruett, R. L. *Science (Washington, D.C.)* **1981**, *211*, 11.
(2) Bailey, D. C.; Langer, S. H. *Chem Rev.* **1981**, *81*, 109.
(3) Brenner, A.; Hucul, D. A. *Inorg. Chem.* **1979**, *18*, 2836.
(4) Brenner, A.; Hucul, D. A.; Hardwick, S. J. *Inorg. Chem.* **1979**, *18*, 1478.
(5) Ballivet-Tkatchenko, D.; Coudurier, G. *Inorg. Chem.* **1979**, *18*, 558.
(6) Hucul, D. A.; Brenner, A. *J. Am. Chem. Soc.* **1981**, *103*, 217.
(7) Commeruc, D.; Chauvin, Y.; Hugues, F.; Basset, J. M.; Olivier, D. *J. Chem. Soc., Chem. Commun.* **1980**, 154.
(8) Geoffroy, G. L.; Wrighton, M. S. "Organometallic Photochemistry"; Academic Press: New York, 1979; p 34 ff.
(9) (a) Nathanson, G.; Gitlin, B.; Rosan, A. M.; Yardley, J. T. *J. Chem. Phys.* **1981**, *74*, 361. (b) Yardley, J. T.; Gitlin, B.; Nathanson, G.; Rosan, A. M. *Ibid.* **1981**, *74*, 370.
(10) Tumas, W.; Gitlin, B.; Rosan, A. M.; Yardley, J. T. *J. Am. Chem. Soc.* **1981**, *104*, 55.
(11) Karny, Z.; Naaman, R.; Zare, R. N. *Chem. Phys. Lett.* **1978**, *59*, 33.
(12) Hellner, L.; Masaret, J.; Vermeil, C. *Nouv. J. Chim.* **1979**, *3*, 721.
(13) A few reports have recently appeared regarding photochemical preparation of supported transition-metal catalysts, See: Nagy, N. B.; Eenoo, M. V.; Derouane, E. G. *J. Catal.* **1979**, *58*, 230. See also: Kinney, J. B.; Staley, R. H.; Reichel, C. L.; Wrighton, M. S. *J. Am. Chem. Soc.* **1981**, *103*, 4273.

0002-7863/82/1504-6590$01.25/0

ondary reactions of a surface-complexed form of the primary photoproduct, $Fe(CO)_4$.

Experimental Section

Chemicals. $Fe_2(CO)_9$ and $Fe_3(CO)_{12}$ were obtained from Strem and were used without further purification. $Fe(CO)_5$, also from Strem, was purified by vacuum transfer to a glass bulb which was kept at liquid-nitrogen temperature except when in use. The bulb was thoroughly degassed before each use. The silica used in most of our experiments was prepared in high purity by Dr. J. N. Armor and Mr. E. J. Carlson of Allied Corp. Silica samples were prepared for use by crushing into particles of ~0.25–0.85-mm diameter (20–60 mesh) and treating at 560 °C in air for ≥2 h. This treatment removes essentially all adsorbed water from the silica surface as shown by IR spectroscopy but leaves a major portion of the surface hydroxyl groups intact, as evidenced by a strong, sharp absorption band at 3750 cm^{-1}. The surface area of the silica employed was 680 $m^2\ g^{-1}$ as measured by the standard BET technique.[14] In one set of experiments, Davison PA-400 silica gel, with a surface area of 740 $m^2\ g^{-1}$, was used as the support. This material was prepared for use as described above.

Apparatus. All gas transfers were handled on a Pyrex vacuum line capable of $\sim 10^{-6}$ torr. Pressures to 1×10^{-3} torr were measured with a capacitance manometer. Lower pressures were measured with an ionization gauge calibrated for nitrogen only. Adsorption experiments were also carried out on this vacuum line using standard differential pressure measurements.[14]

The photolysis cell used in all experiments was a Pyrex cylinder 31 mm i.d. × 100 mm length. The cell was fitted with a greaseless stopcock and had an attached Pyrex finger allowing low-temperature condensation of gases contained in the cell. At each end were 50-mm NaCl windows sealed against the Pyrex cell with Viton O-rings.

Our light source was a Molectron UV-1000 nitrogen laser operated at 1.4 Hz and 4.5 ± 0.5 mJ/pulse. The laser fluence was measured with a calibrated pyroelectric detector before and after each photolysis run. The UV-1000 puts out a rectangular beam of roughly 10 × 30 mm (horizontally elongated), which was vertically expanded with a cylindrical quartz lens to ~30 mm square, providing full coverage of the photolysis cell window.

Gas evolution during photolysis runs was followed with a Varian 3700 gas chromatograph linked to a Varian CDS-111C integrator. The TC detector was calibrated for CO. The column was 5A molecular sieves maintained at 75 °C with a 100 °C injector temperature. Helium was used as the carrier gas, with a flow rate of 30 mL min^{-1}. These conditions allowed good separation between CO and minor impurity gases (N_2, O_2). For qualitative separations of CO and $Fe(CO)_5$, a Chromosorb 102 column was used.

IR spectra were measured on a Perkin-Elmer 283 spectrophotometer. UV–visible spectra were recorded on a Perkin-Elmer 330 spectrophotometer.

Experimental Methods. The silica support material was placed in the photolysis cell such that only those $Fe(CO)_5$ molecules in intimate contact with the support were irradiated. This was accomplished by placing the silica (80 mg) directly onto the inside surface of one of the cell windows and covering with a second, smaller inner NaCl window (25-mm diameter). During experiments in which CO evolution was measured, a germanium inner window was used. The inner window was rigidly held against the cell wall by a 316 stainless steel clamp. This geometry allowed a free space of ~2 mm between the edge of the clamp and the cell wall except at three small contact points, allowing rapid gas diffusion to and from the silica surface at the gas pressures employed. Since the inner window is 6 mm smaller in diameter than the cell, however, roughly 35% of the silica is not clamped between the windows and is thereby removed from the laser path length. In this configuration, ~50 mg of silica is retained, providing a path length of 2.5 mm (transmittance ~25% at 337 nm) over a 25-mm diameter circle. Laser irradiation extending beyond this circle was blocked at the outer cell window. The remaining volume of the cell served as an $Fe(CO)_5$ vapor reservoir, helping to maintain a relatively constant $Fe(CO)_5$ partial pressure during photolysis.

Silica samples, previously heated as described, were very briefly cooled and then placed in the photolysis cell under ambient atmosphere. This process required approximately 5 min after which the cell was evacuated at room temperature. In a few experiments, the silica was cooled under vacuum and transferred to the cell in an inert-atmosphere box under dry argon. This did not change the results of our experiments. After overnight evacuation to $\sim 10^{-5}$ torr, the cell was filled with $Fe(CO)_5$ vapor.

(14) Aveyard, R.; Haydon, D. A. "Introduction to the Principles of Surface Chemistry"; Cambridge University Press: Cambridge, England, 1973; pp 151–177.

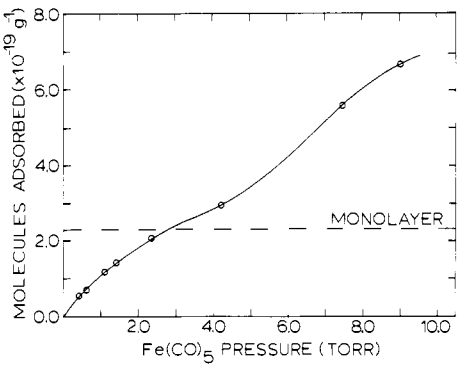

Figure 1. Adsorption isotherm at 29 °C for $Fe(CO)_5$ adsorbed on the silica samples used in the photolysis experiments. The monolayer coverage is estimated.

The vapor was allowed 5 min to equilibrate with the surface before the pressure was recorded and the cell was closed off. It was always observed, however, that much less time was required for the pressure to stabilize (±0.001 torr), indicating efficient equilibration between adsorbed and gas-phase $Fe(CO)_5$ in this cell configuration. All experiments were performed at 29 ± 1 °C.

The amount of CO evolved in the course of a photolysis run was measured after various irradiation intervals by gas chromatography. This was accomplished by thoroughly condensing (−196 °C) the $Fe(CO)_5$ remaining in the cell, prior to filling the GC gas injection loop. After gas sampling with the GC, several minutes were allowed for warming the $Fe(CO)_5$ and reequilibrating it with the silica surface before continuing the photolysis run. The observed quantity of CO was adjusted for the small amount (3%) lost at each successive injection.

IR spectra were occasionally obtained with a second cell, identical with the sample cell, in the spectrometer reference beam. This second cell contained an amount of silica equal to that used in a given photolysis experiment and was identically handled, except for the addition of $Fe(CO)_5$ and subsequent irradiation. The silica background could be equivalently removed from the UV–visible spectra automatically, by subtracting a silica spectrum which had been previously stored in the spectrometer memory just prior to filling the cell with $Fe(CO)_5$.

Results

$Fe(CO)_5$ Adsorption. The adsorption isotherm of $Fe(CO)_5$ on silica was measured to establish the importance of surface interactions in our experiments. Silica samples for adsorption measurements were treated exactly as those in the photolysis experiments. The isotherm obtained at 29 °C is shown in Figure 1. Adsorption is sufficiently extensive that, at equilibrium with the vapor, $Fe(CO)_5$ adsorbed on a given volume of the silica samples used here is roughly 100 times more concentrated than in the same volume of the pure gas. Thus, in our cell design, over half the $Fe(CO)_5$ in the cell and ~99% of the $Fe(CO)_5$ exposed to the laser is adsorbed on the silica surface, independent of the $Fe(CO)_5$ pressure. This interaction is weak however (physisorption), since adsorbed $Fe(CO)_5$ can no longer be detected by IR spectroscopy after evacuation of the cell for less than 5 min.

The adsorption isotherm of $Fe(CO)_5$ on silica (Figure 1) is type II,[14] indicating that saturation does not occur at one monolayer. The approximate first-monolayer coverage can be calculated by using the measured surface area of the silica employed and estimating that an $Fe(CO)_5$ molecule occupies an area of 0.3 nm^2. This estimate, represented by the dashed line in Figure 1, coincides with a knee in the isotherm, which should correspond to first-monolayer coverage.[14] This suggests that overlayers become significant at pressures higher than ~5 torr. These overlayers are probably not well described as additional monomolecular layers dispersed on the silica surface, however, since silica, including the samples employed here, is typically highly microporous. Adsorption above first-monolayer coverage is much more complex in this case. Overlayers on microporous solids are more accurately represented as a three-dimensional liquid phase condensed in the pores.[14]

Photochemistry. Upon photolysis of silica-adsorbed $Fe(CO)_5$, a distinct color change occurs from pale yellow (adsorbed $Fe(CO)_5$) to green. This green product remains after pumping the

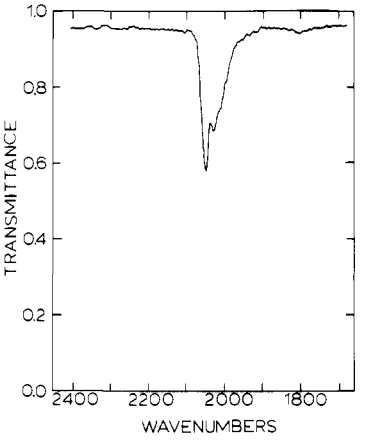

Figure 2. Photolysis product of 2.0 torr $Fe(CO)_5$ on silica following evacuation of unreacted $Fe(CO)_5$. Silica absorption bands have been subtracted.

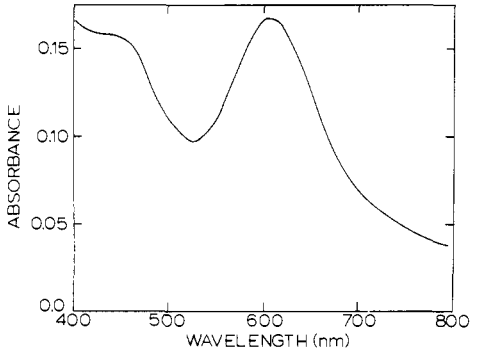

Figure 3. Photolysis product of 2.0 torr $Fe(CO)_5$ on silica following evacuation of unreacted $Fe(CO)_5$. Losses due to support opacity have been subtracted.

cell briefly to 10^{-3} torr but eventually disappears upon continued pumping at pressures below 10^{-4} torr, restoring the appearance and spectrum of the pure silica. The product is stable for several hours at room temperature under an inert atmosphere, finally decomposing to a brown material. Decomposition is faster in air or at elevated temperatures. The product is indefinitely stable at −78 °C under argon.

IR and UV–visible spectra show that the major photolysis product is $Fe_3(CO)_{12}$. This compound can be readily identified by characteristic bands in the carbonyl stretching region of the IR spectrum and by characteristic bands in the visible spectrum. The IR spectrum shown in Figure 2 was obtained after photolysis of 2 torr of $Fe(CO)_5$ in the presence of silica by 1000 shots from the nitrogen laser and removal of the remaining $Fe(CO)_5$ by evacuating the cell for 5 min to 1×10^{-3} torr. This spectrum (2110 vw, 2052 s, 2030 m, 2004 sh, 1800 vw cm^{-1}) agrees well with the solution-phase spectrum of $Fe_3(CO)_{12}$ at 25 °C (nonpolar solvent).[15] Both the IR spectrum and the UV–visible spectrum, shown in Figure 3, match that of a genuine sample of silica-supported $Fe_3(CO)_{12}$, prepared by subliming the complex directly onto the support at 60 °C. IR and UV–visible spectra qualitatively similar to those shown in Figures 2 and 3 are obtained after photolyses carried out at $Fe(CO)_5$ pressures between 0.02 and 3 torr under the same conditions. Spectra obtained after removing unreacted $Fe(CO)_5$ and reirradiating the sample show that photodestruction of the product is negligible under our experimental conditions.

The formation of $Fe_3(CO)_{12}$ as a function of the total laser exposure was followed qualitatively by UV–visible spectroscopy. The $Fe_3(CO)_{12}$ bands grow in monotonically with increasing irradiation and are detectable after the first few laser shots. Changes in the IR spectrum as a function of the total laser exposure cannot

(15) (a) Knight, J.; Mays, M. J. *J. Chem. Soc. D* **1970**, 1006. (b) Cotton, F. A.; Hunter, D. L. *Inorg. Chim. Acta* **1974**, *101*, 273.

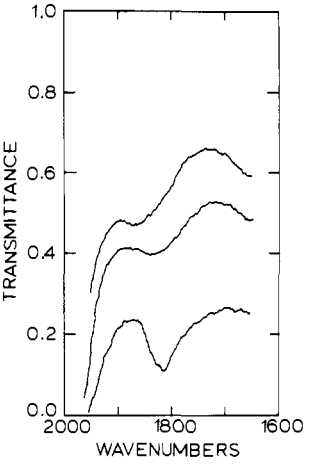

Figure 4. $Fe(CO)_5$ on silica prior to irradiation (top), following photolysis of 5.0 torr $Fe(CO)_5$ (middle), and following photolysis of 10.0 torr $Fe(CO)_5$ (bottom). Note that silica absorption bands were not subtracted.

be similarly followed in the 2100–1950-cm^{-1} region due to the strong absorption of $Fe(CO)_5$ and the long gas-phase path length of our cell, but features in the bridging carbonyl region below 1900 cm^{-1} could be followed. In photolyses carried out at $Fe(CO)_5$ pressures below about 3 torr, only the very weak bridging carbonyl band of $Fe_3(CO)_{12}$ appears in this region at 1800 cm^{-1}. At $Fe(CO)_5$ pressures approaching 5 torr, an additional weak band grows in at 1820 cm^{-1} with increasing irradiation, although this band always disappears after unreacted $Fe(CO)_5$ is removed by pumping out the cell for 5 min to 1×10^{-3} torr. In photolyses carried out at 10 and 16 torr, however, the band at 1820 cm^{-1} is more intense. Figure 4 shows spectra obtained following irradiation at 5 and 10 torr of $Fe(CO)_5$, clearly showing this intensity difference in the 1820-cm^{-1} absorption. In the 10- and 16-torr experiments, the 1820-cm^{-1} band eventually disappears after the cell is pumped out for 5 min and then closed off, but this change requires an additional hour at room temperature. We also found in higher pressure experiments that the sample transparency is greatly reduced during the photolysis. This appears as an increase in the base line absorption levels in both IR and UV–visible spectra recorded after higher pressure photolyses (see Figure 4). The increased opacity also disappears upon briefly pumping out the cell and allowing it to stand for approximately 1 h.

Quantitative data on photolysis product formation is rather difficult to obtain in this system. Spectroscopic information is only semiquantitative due to the imperfect transparency of the support material and the difficulty in accurately preparing standards. We chose to obtain quantitative data by following the evolution of CO by gas chromatography during the course of a photolysis run. Provided the overall reaction induced by the laser is known, measurements of CO evolution can be directly related to the amount of metal carbonyl product formed.

There are a number of potential difficulties in this method, however. For example, CO may be evolved in reactions not initiated by the laser or in reactions not leading to spectroscopically observable (supported metal carbonyl) products. Such reactions include thermal decomposition of $Fe(CO)_5$ or the photoproducts, dissociation of unreacted $Fe(CO)_5$ on the GC column, and irradiation of $Fe(CO)_5$ molecules not in contact with the support. In addition, CO will not be accurately measured if it is adsorbed under our experimental conditions. We have established, however, that these problems are minimal. Thermal decomposition of $Fe(CO)_5$ on silica is negligible at room temperature, as evidenced by insignificant CO evolution in nonirradiated control runs over periods equal to those of the longest photolysis runs. Also, the amount of CO detected after a given laser exposure remains unchanged after an additional period in the dark, indicating that CO evolution arising from photoproduct thermal decomposition is negligible over the time period of these measurements. $Fe(CO)_5$ is indeed decomposed on the molecular sieve GC column, yielding 5 mol of CO detected per mol of $Fe(CO)_5$, but we precluded its

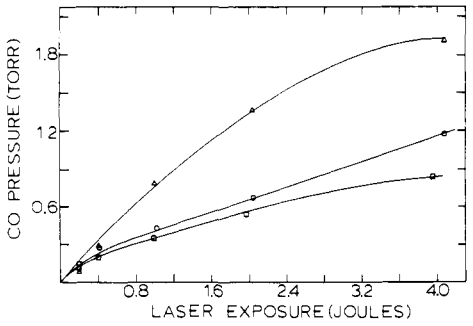

Figure 5. CO evolved during photolysis of silica-adsorbed $Fe(CO)_5$ at pressures of 2 (□), 5 (△), and 10 torr (○).

loss from the cell during a gas injection by condensing it into the cell side arm. The efficiency of this condensation is shown by the negligible quantity of CO observed in chromatograms recorded prior to irradiation. This also suggests that sampling the gas-phase contents of the cell during the course of a photolysis run does not appreciably change the $Fe(CO)_5$ pressure. Significant contributions from nonsurface photoreactions can also be ruled out, since the geometry of our cell was chosen to minimize irradiation of $Fe(CO)_5$ molecules not adsorbed on the silica surface. We prevented light from passing through the sample and into the gas-phase region of the cell by using a germanium flat as the inner window in runs where CO evolution was measured. Last, we find that CO adsorption on silica is negligible at 29 °C.

One remaining uncertainty in these measurements is the effect of introducing impurities by opening the cell to the evacuated GC injection system in the course of a photolysis run. Minute quantities of N_2 and O_2 were detected in the chromatograms, indicating that some air may have entered the cell. Although the effect of oxygen on the photochemistry is not fully known, we did not observe any spectroscopic differences between runs that were sampled by GC and those that were not. We also found no discrepancy in the amount of CO evolved during runs in which the cell was sampled as many as six times vs. those in which it was sampled only once at the end of the run.

The amount of CO evolved as a function of the integrated laser exposure in joules was measured for photolyses carried out at 2, 5, and 10 torr, respectively. Representative CO evolution data from single runs are shown in Figure 5. The precision of the data is estimated to be within ±1% on the basis of the reproducibility of the integrator response to known quantities of CO and the single-point calibration of the detector response performed after each run. The accuracy is lower, as demonstrated by the reproducibility of the actual data, but we estimate that it is within ±20%. In every case the relative positions of the CO evolution curves obtained in runs performed at different $Fe(CO)_5$ pressures are reproduced.

In one set of experiments, Davison PA-400 silica gel was used as the support. Photolysis of $Fe(CO)_5$ adsorbed on this type of silica again yields $Fe_3(CO)_{12}$ as the only significant photoproduct. The Davison silica is reasonably transparent but is more dense than the silica used in most of our experiments. The higher bulk density translates into a higher concentration of $Fe(CO)_5$ exposed to the laser at a given surface coverage. Under these conditions, it was difficult to prevent total absorption of the laser output, even at surface coverages well below one monolayer. This problem could obviously be circumvented by using a thinner sample, but this is less desirable for our experiments than use of a lower density silica, since our path length is already quite short (~2.5 mm). Smaller silica particles were used in a few experiments to reduce the path length, but this resulted in greatly increased light scattering. Compressed silica pellets were also unsatisfactory, since we could not be certain of rapid equilibration between gas-phase and adsorbed $Fe(CO)_5$.

Discussion

The photochemistry of $Fe(CO)_5$ has been extensively studied in both the gas phase and in condensed media. The primary photochemical step[16,17] involves loss of CO according to reaction 1. If irradiation of $Fe(CO)_5$ is carried out in the presence of added

$$Fe(CO)_5 \xrightarrow{h\nu} Fe(CO)_4 + CO \quad (1)$$

ligands, photosubstitution takes place as in reaction 2, provided

$$Fe(CO)_4 + L \rightarrow Fe(CO)_4L \quad (2)$$

the substituted complex is stable under the reaction conditions. If no additional reactants are present, irradiation of $Fe(CO)_5$ in the gas[18] or liquid phase[19] or in solution[20] yields predominantly $Fe_2(CO)_9$. This presumably occurs by a two-step process, with reaction 3 following reaction 1.[16] The $Fe_2(CO)_9$ forms as a solid

$$Fe(CO)_4 + Fe(CO)_5 \rightarrow Fe_2(CO)_9 \quad (3)$$

in each case, either coating the cell walls during photolysis of $Fe(CO)_5$ in the gas phase or precipitating during photolysis of $Fe(CO)_5$ in the liquid or solution phase, and is thereby removed from the reaction.

We do not expect that the primary photochemistry of silica-adsorbed $Fe(CO)_5$ will significantly differ from that observed in homogeneous systems. Thus, if silica participates only as an inert support, $Fe_2(CO)_9$ is the photoproduct expected upon photolysis of adsorbed $Fe(CO)_5$. In contrast, we find that the only abundant photoproduct is $Fe_3(CO)_{12}$, as confirmed by both IR and UV–visible spectroscopy. From the IR spectrum alone, we can be certain that $Fe_2(CO)_9$ is not a major product, as the $Fe_2(CO)_9$ spectrum[21] exhibits a strong bridging carbonyl band at ~1830 cm^{-1}. We observed a broad band centered at 1820 cm^{-1} in the higher pressure experiments, but it was always weak compared to the $Fe_3(CO)_{12}$ terminal carbonyl bands. This feature at 1820 cm^{-1} and its assignment will be discussed later.

Our results thus imply that silica may not act as an inert support during the photolysis of $Fe(CO)_5$. This is reasonable, since silica surface hydroxyl groups and siloxane bridging oxygen atoms should be good electron donors capable of acting as ligands toward iron. This suggests that reactions 1 and 2 will result in the formation of $Fe(CO)_4(SiO_2)$, which represents a complex that is bound to the surface via one of these groups. The interaction of $Fe(CO)_4$ with these surface groups will be relatively weak, however, as neither the surface hydroxyl groups nor the siloxane bridging oxygen atoms can stabilize the metal–ligand bond by accepting electrons back into a π system. $Fe(CO)_4(SiO_2)$ might thus be modeled reasonably well by $Fe(CO)_4(THF)$ (THF = tetrahydrofuran), which is reactive toward thermal substitution by added ligands under very mild conditions, suggesting a weak $Fe(CO)_4$–THF bond.[22]

In an attempt to observe $Fe(CO)_4(SiO_2)$, we have recently undertaken a study of silica-adsorbed $Fe(CO)_5$ photochemistry at reduced temperatures and low surface coverages.[27] Photolysis

(16) Wrighton, M. *Chem. Rev.* **1974**, *74*, 401.
(17) Nathanson et al. have shown[9] that absorption of a single UV photon by $Fe(CO)_5$ in the gas phase can induce the loss of several CO ligands, giving high quantum yields of $Fe(CO)_3$ and $Fe(CO)_2$. This involves dissociation of excited $Fe(CO)_4$, which retains much of the initial energy following reaction 1. This behavior is not manifested in condensed media nor in the gas phase at higher $Fe(CO)_5$ concentrations and should also be unimportant in our experiments if the silica surface efficiently quenches $Fe(CO)_4$.
(18) Chisolm, M. H.; Massey, A. G.; Thompson, N. R. *Nature (London)* **1966**, *211*, 67.
(19) Dewar, J.; Jones, H. O. *Proc. R. Soc. London, Ser. A* **1905**, *76*, 558.
(20) Braye, E. H.; Huebel, W. *Inorg. Synth.* **1966**, *8*, 178.
(21) Kristoff, J. S.; Shriver, D. F. *Can. J. Spectrosc.* **1974**, *19*, 156.
(22) (a) Strohmeier, W. *Angew. Chem., Int. Ed. Engl.* **1964**, *3*, 730. Reactions involving iron carbonyls in THF may be complicated by electron-transfer processes leading to the formation of paramagnetic species.[26] (b) Cotton, F. A. *Prog. Inorg. Chem.* **1976**, *21*, 1.
(23) Schubert, E. H.; Sheline, R. K. *Inorg. Chem.* **1966**, *5*, 1071.
(24) Koerner von Gustorf, E.; Henry, M. C.; DiPetro, C. *Z. Naturforsch. B* **1966**, *B21*, 42.
(25) Birencwaig, F.; Shamai, H.; Shvo, Y. *Tetrahedron Lett.* **1979**, 2947.
(26) Dawson, P. A.; Peake, B. M.; Robinson, B. H.; Simpson, J. *Inorg. Chem.* **1980**, *19*, 465.

at 100–150 K leads to the growth of CO stretching bands at ~1960 and ~1940 cm^{-1}, belonging to a species that is thermally unstable above 150 K but indefinitely stable at 100 K. These bands are assigned to $Fe(CO)_4(SiO_2)$ by comparison with bands observed for $Fe(CO)_4(THF)$ at 1963 and 1946 cm^{-1}.[28] The bands we observed cannot belong to free $Fe(CO)_4$, as this species is quite unstable in a matrix at 50 K in the presence of small amounts of CO. Other unstable iron carbonyl species (e.g., $Fe_2(CO)_8$, $Fe_2(CO)_8(SiO_2)$, $Fe(CO)_3$) are not expected to exhibit IR bands in this region. We also found that thermal dissociation of this unstable species in the dark above 150 K leads to growth of bands attributed to $Fe_3(CO)_{12}$. No bands attributable to $Fe_2(CO)_9$ were observed by IR spectroscopy.

Based on a comparison of the $Fe(CO)_5$ photochemistry observed on a silica surface with that observed in solution, the participation of silica surface groups as weak ligands provides a rationale for the formation of $Fe_3(CO)_{12}$ in our experiments. In solutions containing a weak ligand, reactions 1 and 2 yield the monosubstituted product $Fe(CO)_4L$, which is unstable and is not isolated. While thermal reaction of this product complex might be expected to yield $Fe_2(CO)_9$ via reaction 3, $Fe_3(CO)_{12}$ is formed instead.[23,24] The absence of $Fe_2(CO)_9$ is explained by its instability under these conditions, since $Fe_2(CO)_9$ dissociates in solution in the presence of a weak ligand, yielding $Fe_3(CO)_{12}$ and $Fe(CO)_5$. The intermediate leading to formation of $Fe_3(CO)_{12}$ in this thermal reaction is again the unstable mononuclear species, $Fe(CO)_4L$.[22b,25,26] It thus appears that unstable $Fe(CO)_4L$ complexes, whether produced photochemically from $Fe(CO)_5$ or thermally from $Fe_2(CO)_9$, react to give $Fe_3(CO)_{12}$ in solution.

Since silica surface groups can apparently act as weak ligands, these solution-phase results suggest that $Fe_3(CO)_{12}$ could be expected as a photoproduct in our experiments. Similarly, the instability of $Fe_2(CO)_9$ in the presence of weak ligands explains why that species is not a significant product. In an attempt to prepare silica-supported $Fe_2(CO)_9$, we sublimed the finely divided pure solid onto silica in a closed tube under mild conditions (40 °C, background pressure ~10^{-6} torr). While $Fe_2(CO)_9$ normally sublimes without dissociation under these conditions,[18] the IR spectrum of the silica-supported product shows no evidence of $Fe_2(CO)_9$ but only bands attributable to $Fe_3(CO)_{12}$ and $Fe(CO)_5$. In addition, $Fe(CO)_5$ and CO were detected in the tube by gas chromatography. This reaction thus appears to be analogous to the reaction of $Fe_2(CO)_9$ in solutions containing a weak ligand.

The parallel between the $Fe(CO)_5$ chemistry observed on a silica surface and that observed in solution suggests that the mechanism for the formation of $Fe_3(CO)_{12}$ could be the same in both cases. The mechanism operating in solution is not fully understood, but it has been suggested that $Fe_3(CO)_{12}$ is formed via trimerization of $Fe(CO)_4L$ or solvated $Fe(CO)_4$, produced by thermal dissociation of $Fe(CO)_4L$.[22b] It is difficult, however, to compare this solution-phase trimerization with a similar process occurring on a surface, since $Fe(CO)_4(SiO_2)$ is a bound species which cannot trimerize without dissociating. A strict analogy with the solution-phase process requires the $Fe(CO)_4$–SiO_2 bond to be weak, so that $Fe(CO)_4$ can be sufficiently mobile on the surface to undergo trimerization. Migration of surface species has been extensively studied,[29–31] but it is not possible to estimate the mobility of $Fe(CO)_4$ using any of the present theoretical models of surface migration without knowing the strength of the bond between $Fe(CO)_4$ and the surface ligating group. Facile surface trimerization of $Fe(CO)_4$ at room temperature is not unreasonable, however, since it is often found that barriers to migration of chemically adsorbed molecules represent only a fraction of the actual binding energy between the adsorbed molecule and the surface.[31,32] It is also likely that trimerization of $Fe(CO)_4$ in any medium will proceed at a nearly encounter-controlled rate, since the formation of $Fe_3(CO)_{12}$ from $Fe(CO)_4$ has been observed in a matrix at 20 K. Thus, we propose the mechanism outlined in Scheme I as the simplest explanation for the formation of $Fe_3(CO)_{12}$ in our experiments.

Scheme I

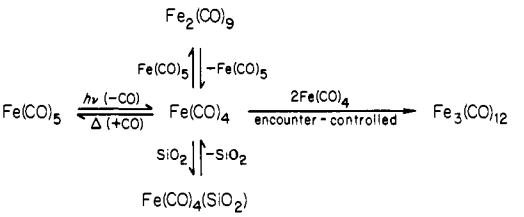

Scheme II

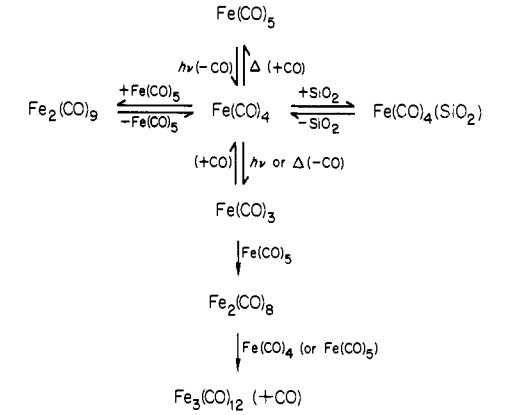

This scheme provides a reasonable explanation for our results, but we also consider a pathway involving formation of $Fe_3(CO)_{12}$ via an $Fe(CO)_3$ intermediate. This species could be important, since thermal dissociation of solvated $Fe(CO)_4$ to $Fe(CO)_3$ and CO is believed to be quite facile at room temperature. Evidence for this is provided by the observation of $Fe(CO)_3L_2$ upon single-photon dissociation of $Fe(CO)_5$ in solutions containing triphenylphosphine (L = PPh_3).[34] Additional evidence comes from the solution-phase kinetic work of Cardaci[35] and of Braterman and Wallace.[36] Indeed, Engelking and Lineberger have suggested that the $Fe(CO)_3$–CO bond strength is only 5 kcal/mol^{-1}, although the uncertainty in their measurement is large.[37] In addition, secondary photochemical formation of $Fe(CO)_3$ must be considered, since photodissociation of matrix-isolated $Fe(CO)_4$ to $Fe(CO)_3$ has been observed.[17,38] Thermal or photochemical formation of $Fe(CO)_3$ could lead to $Fe_3(CO)_{12}$ as simply outlined

(27) Trusheim, M. R.; Jackson, R. L., to be submitted for publication.
(28) Black, J. D.; Braterman, P. G. *J. Organomet. Chem.* **1975**, *85*, C7.
(29) Barrer, R. M. In "The Solid-Gas Interface"; Flood, E. A., Ed.; Marcel Dekker: New York, 1967; pp 557–609.
(30) Tompkins, F. C. "Chemisorption of Gases on Metals"; Academic Press: London, 1978; pp 261–269.
(31) Ehrlich, G.; Stolt, K. *Annu. Rev. Phys. Chem.* **1980**, *31*, 603.
(32) Sladek, K. J.; Gilliland, E. R.; Baddour, R. F. *Ind. Eng. Chem. Fundam.* **1974**, *13*, 100.
(33) Poliakoff, M.; Turner, J. J. *J. Chem. Soc., Dalton Trans.* **1974**, 2276.
(34) Schroeder, M. A.; Wrighton, M. S. *J. Am. Chem. Soc.* **1976**, *98*, 551.
(35) (a) Cardaci, G. *Inorg. Chem.* **1974**, *13*, 368. (b) Cardaci, G. *Ibid.* **1974**, *13*, 2974.
(36) Braterman, P. S.; Wallace, W. J. *J. Organomet. Chem.* **1973**, *30*, C17.
(37) Engelking, P. C.; Lineberger, W. C. *J. Am. Chem. Soc.* **1979**, *101*, 5569. This bond dissociation energy was calculated from the thermochemical cycle

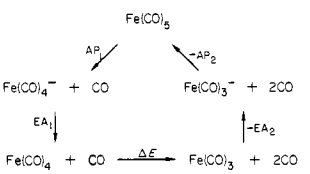

where AP = appearance potential and EA = electron affinity. Appearance potentials, however, do not provide differences between thermodynamic state functions when the dissociation processes involved are exoergic or have barriers. Both of these problems may affect the above cycle, so we approach the calculated bond dissociation energy of $Fe(CO)_4$ with caution.
(38) Poliakoff, M. *J. Chem. Soc., Dalton Trans.* **1974**, 210.
(39) See, however: Fischler, I.; Hildenbrand, K.; Koerner von Gustorf, E. *Angew. Chem., Int. Ed. Engl.* **1975**, *14*, 54.

in Scheme II. The last two reactions leading to $Fe_3(CO)_{12}$ are unprecedented, as reactions of both $Fe(CO)_3$ and $Fe_2(CO)_8$ are unknown,[38] but we believe that they provide a reasonable pathway by which $Fe(CO)_3$ could lead to $Fe_3(CO)_{12}$.

We note, however, that in the absence of secondary photochemistry both pathways for $Fe_3(CO)_{12}$ formation require at least transient formation of uncomplexed $Fe(CO)_4$ on the silica surface via thermal dissociation of $Fe(CO)_4(SiO_2)$. In Scheme I, surface migration of $Fe(CO)_4$ most likely occurs by a dissociation–recombination mechanism involving surface site to site jumps of free $Fe(CO)_4$.[29-31] In Scheme II, thermal formation of $Fe(CO)_3$ from $Fe(CO)_4(SiO_2)$ is expected to proceed stepwise via an $Fe(CO)_4$ intermediate.[35] Once formed, $Fe(CO)_4$ is much more likely to undergo rapid recombination with another surface ligand site than to dissociate further to $Fe(CO)_3$ and CO, unless this dissociation barrier is nearly zero. Without secondary photochemistry, Scheme I thus appears to offer a better explanation for the formation of $Fe_3(CO)_{12}$ on the silica surface. While we cannot rule out secondary photochemical formation of $Fe(CO)_3$ in our experiments, Poliakoff and Turner have shown that weakly complexed forms of $Fe(CO)_4$ have an absorption maximum reasonably far removed from the wavelength of our laser light source.[40] We also note that our overall conversion of $Fe(CO)_5$ was always less than 15% (see below) and that our laser fluence was well below the fluence threshold for single laser pulse two-photon photochemistry previously observed for gas-phase $Fe(CO)_5$.[9]

A pathway that must also be considered here involves $Fe_2(CO)_9$ as the dinuclear intermediate in the oligomerization process leading to $Fe_3(CO)_{12}$. Since there is no evidence that $Fe_2(CO)_9$ reacts directly with $Fe(CO)_5$ or with ligands by an associative mechanism, this pathway must involve one of two processes: (1) prior dissociation of $Fe_2(CO)_9$ to $Fe_2(CO)_8$ or (2) reaction of $Fe_2(CO)_9$ with $Fe(CO)_4$ or $Fe(CO)_3$. The first process is unlikely since substituted complexes of the form $Fe_2(CO)_8L$ have not been observed in thermal reactions of $Fe_2(CO)_9$ in the presence of ligands. Instead, mononuclear products are formed. Since these ligand substitution reactions probably occur by a dissociation–recombination mechanism, the lowest energy dissociation pathway of $Fe_2(CO)_9$ appears to result in $Fe(CO)_4$ and $Fe(CO)_5$, not $Fe_2(CO)_8$ and CO. Photochemical dissociation of $Fe_2(CO)_9$ to $Fe_2(CO)_8$ has been reported,[41] but this photoreaction could not be induced by 333-nm light, very close to our N_2 laser wavelength of 337 nm. The second process above is more reasonable, but only if $Fe_2(CO)_9$ is stable on silica, since dissociation into $Fe(CO)_4$ and $Fe(CO)_5$ is not consistent with this alternative pathway. We have shown, however, that it is not stable. Thus, the formation of $Fe_3(CO)_{12}$ in our experiments is not satisfactorily explained by invoking $Fe_2(CO)_9$ as the dinuclear intermediate.

Pressure Dependence. The photochemistry of silica-adsorbed $Fe(CO)_5$ is quite clean at $Fe(CO)_5$ pressures below ~3 torr. The only photoproduct is $Fe_3(CO)_{12}$; IR bands attributable to $Fe_2(CO)_9$ are not observed. Complications arise at higher pressures, however. A weak absorption at 1820 cm^{-1} is observed in photolyses carried out at $Fe(CO)_5$ pressures of 5 torr, and this band is more intense in runs performed at 10 and 16 torr. In addition, the samples in the 10- and 16-torr photolyses lose transparency during the course of a run. This is manifested in the IR and UV–visible spectra as an increasd base line absorption, suggesting that the opacity is due to increased light scattering. These changes reproducibly occur only in the higher pressure photolyses.

Examination of the adsorption isotherm (Figure 1) indicates that the onset of this behavior coincides with the transition from approximately single-monolayer coverage to substantially higher coverage. At 5 torr, the surface coverage of $Fe(CO)_5$ appears to be somewhat greater than one monolayer, and at 10 and 16 torr, over half of the $Fe(CO)_5$ resides in molecular overlayers. As discussed earlier, these overlayers are not describable in terms of stacked two-dimensional structures but are much more accurately represented as a three-dimensional liquid phase.[14] This suggests that at higher $Fe(CO)_5$ pressures where this liquid phase is important, different photochemical behavior might be expected. Photolysis of $Fe(CO)_5$ in the first monolayer, which is intimately associated with the surface, should lead to $Fe_3(CO)_{12}$. Photolysis of $Fe(CO)_5$ in the liquid overlayers should lead to $Fe_2(CO)_9$ as has been previously observed[20] in photolysis of pure liquid $Fe(CO)_5$. Any $Fe_2(CO)_9$ formed in the overlayers can migrate to the surface, where it is converted to $Fe_3(CO)_{12}$ and $Fe(CO)_5$, or it can aggregate to give solid $Fe_2(CO)_9$.

This simple two-phase model is consistent with our observations in the higher presure photolyses. The 1820-cm^{-1} band can be assigned to the bridging carbonyl stretch of $Fe_2(CO)_9$.[21] Loss of transparency can be explained by the aggregation of photochemically formed $Fe_2(CO)_9$ in the $Fe(CO)_5$ overlayers. This model also satisfactorily explains why both the 1820-cm^{-1} absorption and the opacity disappear upon briefly pumping out the cell and allowing it to stand at room temperature. Removal of adsorbed $Fe(CO)_5$ by pumping will quickly dislodge the overlayers, leaving aggregated $Fe_2(CO)_9$ on the silica surface where it can eventually be converted to $Fe_3(CO)_{12}$ and $Fe(CO)_5$ as previously noted.

CO Evolution. The amount of CO evolved can be related to the amount of adsorbed $Fe(CO)_5$ consumed if the overall stoichiometry of the photoreaction is known. Our spectroscopic data show that $Fe(CO)_5$ is mostly consumed in the reaction

$$3Fe(CO)_5 \rightarrow Fe_3(CO)_{12} + 3CO \qquad (4)$$

so that one molecule of CO is evolved per $Fe(CO)_5$ molecule consumed. Since the amount of $Fe(CO)_5$ consumed in other reactions is apparently small, an assumption that one CO is evolved per $Fe(CO)_5$ consumed should be good, especially in light of the relatively large error in the actual data (±20%).

We can, therefore, use these data to calculate the extent of $Fe(CO)_5$ conversion at a given integrated laser exposure. A conversion of 11 ± 2% is found at an integrated laser exposure of 4 J for photolyses performed at $Fe(CO)_5$ pressures of both 2 and 5 torr, while the 10-torr data shows a conversion of 3 ± 1% for the same exposure. The much lower conversion found in the 10-torr data can be explained by the loss of transparency observed in the 10-torr samples. This effectively reduces the rate of photon absorption by $Fe(CO)_5$ in the higher pressure experiments.

The rate of CO evolution declines rapidly with increased laser exposure at all pressures, however. This falloff occurs at conversions below 10%, indicating that it is not due to the loss of $Fe(CO)_5$. The best explanation for this falloff at such low conversions is that the photoproduct, $Fe_3(CO)_{12}$, absorbs much more strongly than $Fe(CO)_5$ at 337 nm but is not appreciably photoreactive.[43] This results in a reduced rate of $Fe(CO)_5$ absorption and, thus, in a reduced rate of photolysis.

We had hoped to use the CO evolution data to determine more definitively the reaction mechanism involved in our experiments, since different mechanisms call for different quantum yields of CO. If photodissociation of $Fe(CO)_5$ to $Fe(CO)_4$ and CO is unit efficient on the silica surface, as it is in solution,[16] Scheme I requires a CO quantum yield of 1, while Scheme II calls for a CO quantum yield of up to 3. It is not possible to measure the quantum yield accurately, however, since light scattering and reflection by the silica as well as absorption by the photoproduct do not allow a determination of the number of photons absorbed by $Fe(CO)_5$. There are additional problems involving the sample inhomogeneity. We note only that a tangent taken at the origin of Figure 5 for the 5-torr data, where nearly complete absorption of incident photons by $Fe(CO)_5$ should be approached, suggests an approximate initial yield of 0.9 (±~0.2) molecule of CO evolved per incident photon.

Conclusion

We have prepared silica-supported $Fe_3(CO)_{12}$ in a single step via nitrogen laser irradiation of $Fe(CO)_5$ adsorbed on the silica

(40) Poliakoff, M. *Chem. Soc. Rev.* **1978**, *7*, 527.
(41) Poliakoff, M.; Turner, J. J. *J. Chem. Soc. A* **1971**, 2403.
(42) Dahl, L. F.; Rundle, R. E. *J. Chem. Phys.* **1957**, *27*, 323.
(43) Graff, J. L.; Sanner, R. D.; Wrighton, M. S. *J. Am. Chem. Soc.* **1979**, *101*, 273.

surface. Under conditions where the surface coverage of $Fe(CO)_5$ does not exceed one monolayer, $Fe_3(CO)_{12}$ is the only photoproduct observed spectroscopically. If the surface coverage of $Fe(CO)_5$ greatly exceeds one monolayer, $Fe_2(CO)_9$ is also an important product and appears to be aggregated rather than dispersed on the support surface. The mechanism for the formation of $Fe_3(CO)_{12}$ appears to involve the initial formation of surface-bound $Fe(CO)_4$, which undergoes subsequent thermal trimerization on the silica surface.

Acknowledgment. We would like to thank Dr. J. T. Yardley for many helpful discussions. We also thank Dr. John Armor and Mr. Emery J. Carlson for preparation of the silica samples and Ms. Suzanne Kowalski for helpful analytical work.

Registry No. $Fe(CO)_5$, 13463-40-6; $Fe_3(CO)_{12}$, 17685-52-8; CO, 630-08-0; silica, 7631-86-9.

Bis(1-methyluracilato-N^3)-*cis*-diammineplatinum(II)-4-Water and Bis(μ-1-methyluracilato-N^3,O^4)-*cis*-diammineplatinum(II)diaquocopper(II) Sulfate-4.5-Water (Head-Head). Preparation, Crystal Structures, and Implications for the Formation of Heteronuclear Pt,M Complexes

Dietmar Neugebauer and Bernhard Lippert*

Contribution from the Anorganisch-Chemisches Institut der Technischen Universität München, 8046 Garching, FRG. *Received February 24, 1982*

Abstract: The syntheses and crystal structures of two complexes of 1-methyluracil are reported. *cis*-$Pt(NH_3)_2(1\text{-}MeU)_2\cdot 4H_2O$ (**2**) crystallizes in space group $C2/c$ with cell parameters a = 26.822 (14) Å, b = 7.030 (2) Å, c = 20.044 (9) Å, and β = 96.36 (4)° and has eight formula units in the unit cell. The structure was refined on 2416 reflections to R_1 = 0.038 and R_2 = 0.044. 1-Methyluracil anion ligands, 1-MeU, exhibit N3 platinum binding and are arranged in head-tail fashion. With Cu(II), **2** forms heteronuclear complexes of Pt:Cu = 1:1 and 2:1 stoichiometries, depending upon the applied Pt:Cu ratio *and* the anions present. The crystal structure of one of these complexes has been determined. *cis*-$[Pt(NH_3)_2(1\text{-}MeU)_2Cu(H_2O)_2]SO_4\cdot 4.5H_2O$ (**4**) crystallizes in space group $P\bar{1}$ with cell parameters a = 10.398 (10) Å, b = 10.773 (8) Å, c = 11.772 (9) Å, α = 102.88 (6)°, β = 102.62 (7)°, and γ = 105.05 (7)° and has two formula units in the unit cell. The structure was refined on 3028 reflections to R_1 = 0.091 and R_2 = 0.096. Pt and Cu have square-planar coordination spheres and are linked through two 1-MeU ligands in a head-head arrangement, binding to Pt via N3 and to Cu via O4. The coordination spheres are completed by two NH_3 ligands (Pt) and two H_2O groups (Cu), each in cis arrangements. The Pt-Cu distance within the cation is 2.765 (3) Å. Related heteronuclear Pt,Cu complexes of 2:1 stoichiometries and varying anions have been prepared and reasons for their formation are discussed. Possibilities for the formation of homonuclear Pt_x and heteronuclear Pt_x,M_y complexes with long metal chains are outlined.

Introduction

1-Methyluracil can be considered a model of the naturally occurring RNA base uridine and the DNA base thymidine. Its metal coordination properties, like those of the other nucleic acid components, are of interest with respect to nucleic acid replication,[1] mutagenesis,[2] carcinogenesis,[3] antitumor activity,[4] and heavy-metal labeling of nucleic acids.[5] N1-substituted uracil contains several potential donor atoms for metal coordination—N3, O4, O2, C5, and combinations of these[6-10] —most of which are documented in the literature (Chart I). With unsubstituted uracil the number of possible coordination sites is even larger.[11] Recently, we made extensive use of the excellent ligating properties of N3-platinated pyrimidine-2,4-diones via their exocyclic oxygen atoms, specifically of complexes of composition *cis*-$Pt(NH_3)_2(1\text{-}MeU)_2$ and *cis*-$Pt(NH_3)_2(1\text{-}MeT)_2$,[12] which lead to di-[13] and heteronuclear Pt,M

Chart I

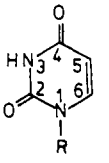

(1) Eichhorn, G. L. *Met. Ions Biol. Syst.* **1980**, *10*, 1-21 and references therein.
(2) Loeb, L. A.; Zakour, R. A. In "Nucleic Acid-Metal Ion Interactions"; Spiro, T. G., Ed.; Wiley: New York, 1980; Vol. 1, pp 117-144.
(3) Flessel, C. P.; Furst, A.; Radding, S. B. *Met. Ions Biol. Syst.* **1980**, *10*, 23-54 and references therein.
(4) See, e.g.: (a) Prestayko, A. W., Crooke, S. T., Carter, S. K., Eds. "Cisplatin-Current Status and New Developments"; Academic Press: New York, **1980**. (b) Roberts, J. J.; Thomson, A. J. *Prog. Nucleic Acid Res. Mol. Biol.* **1979**, *22*, 71. (c) Rosenberg, B. *Met. Ions Biol. Syst.* **1980**, *11*, 127-196.
(5) Barton, J. K.; Lippard, S. J. In "Nucleic Acid-Metal Ion Interactions"; Spiro, T. G., Ed.; Wiley: New York, 1980; Vol. 1, pp 33-113.
(6) Mansy, S.; Tobias, R. S. *Inorg. Chem.* **1975**, *14*, 287.
(7) (a) Cartwright, B. A.; Goodgame, M.; Johns, K. W.; Skapski, A. C. *Biochem. J.* **1978**, *175*, 337. (b) Goodgame, M.; Johns, K. W. *Inorg. Chim. Acta* **1978**, *30*, L335.
(8) Faggiani, R.; Lock, C. J. L.; Pollock, R. J.; Rosenberg, B.; Turner, G. *Inorg. Chem.* **1981**, *20*, 804.
(9) Lippert, B.; Neugebauer, D. *Inorg. Chem.* **1982**, *21*, 451.
(10) Dale, R. M. K.; Martin, E.; Livingston, D. C.; Ward, D. C. *Biochemistry* **1975**, *14*, 2447.
(11) Lippert, B. *Inorg. Chem.* **1981**, *20*, 4326.
(12) Abbreviations used: 1-MeU = monoanion of 1-methyluracil; 1-MeT = monoanion of 1-methylthymine; 1-MeUH = neutral 1-methyluracil.

0002-7863/82/1504-6596$01.25/0